Monitoring groundwater fluxes variations through active-DTS measurements

Nataline Simon, Olivier Bour, Nicolas Lavenant, Gilles Porel, Benoît Nauleau, Maria Klepikova

Journal Pre-proofs

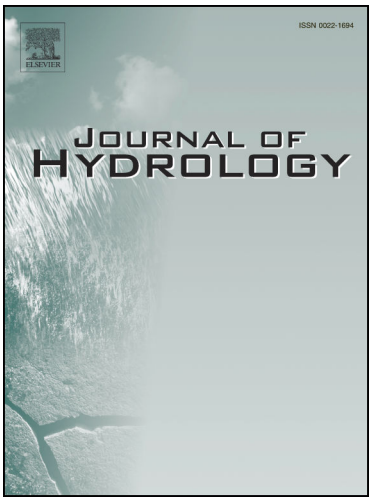

Research papers

Monitoring groundwater fluxes variations through active-DTS measurements

Nataline Simon, Olivier Bour, Nicolas Lavenant, Gilles Porel, Benoît Nauleau, Maria Klepikova

PII: S0022-1694(23)00697-2
DOI: https://doi.org/10.1016/j.jhydrol.2023.129755
Reference: HYDROL 129755

To appear in: *Journal of Hydrology*

Received Date: 17 October 2022
Revised Date: 17 February 2023
Accepted Date: 26 May 2023

Please cite this article as: Simon, N., Bour, O., Lavenant, N., Porel, G., Nauleau, B., Klepikova, M., Monitoring groundwater fluxes variations through active-DTS measurements, *Journal of Hydrology* (2023), doi: https://doi.org/10.1016/j.jhydrol.2023.129755

Monitoring groundwater fluxes variations through active-DTS measurements

Nataline Simon[1,2], Olivier Bour[1], Nicolas Lavenant[1], Gilles Porel[3], Benoît Nauleau[3] and Maria Klepikova[1]

[1] Univ Rennes, CNRS, Géosciences Rennes – UMR 6118, Rennes, France

[2] Department Urban and Environmental Engineering, Hydrogeology and Environmental Geology, Liège Université, Building B52, 4000 Sart Tilman, Belgium (Present address)

[3] Department of Earth Sciences, IC2MP UMR 7285, Université de Poitiers, CNRS, HydrASA, Poitiers, France

Corresponding author: Nataline Simon (nataline.simon2@gmail.com)

Abstract

Considering the need of characterizing temporal dynamic of groundwater and the lack of available methods, we investigate the feasibility of active-Distributed Temperature Sensing (DTS) measurements to monitor and quantify groundwater fluxes variations over time. Active-DTS, which consists here of heating a Fiber Optic (FO) cable and in monitoring the temperature elevation, has proven to be very efficient to quantify the spatial distribution of groundwater fluxes in saturated porous media at high resolution with low uncertainties. However, the approach has never been tested to continuously monitor groundwater fluxes changes. To test this, we rely on both numerical simulations and sandbox experiments to assess the sensitivity of temperature elevation to variable flow conditions and our ability to interpret associated temperature variations. Results confirm that the temperature elevation and evolution over time is sensitive to flow conditions and that associated temperature variations can be used to characterize groundwater fluxes variations. First, experimental and numerical results show that when a flow change is followed by a long-enough steady-state flow period the temperature stabilizes independently of previous fluxes conditions. In such case, the stabilization temperature can easily be interpreted to estimate groundwater fluxes using the analytical model commonly used under steady flow conditions to interpret active-DTS measurements. Furthermore, we demonstrate here that, under certain flow conditions depending on the nature of flow variations, the approach offers the possibility of continuously monitoring fluxes variations. For instantaneous flow changes, it is even possible to go further by reproducing temperature signal variations over time by applying the superposition principle to the analytical model. In the end, these preliminary tests are particularly promising and open new perspectives for monitoring and/or quantifying the temporal dynamic of groundwater fluxes at different temporal scales including diurnal and short-term periodic fluxes variations.

Keywords : Groundwater flow monitoring; Groundwater dynamics; Heat tracer experiment; Active-DTS; Heated Fiber Optic Cable

1. Introduction

The characterization of groundwater fluxes is challenging in many hydrogeological contexts (Hermans et al. 2022), in particular for characterizing the temporal variabilities of flows at compartment interfaces, which remains particularly critical. For instance, in coastal sediments, transient flow conditions influence the ecosystem productivity and its biogeochemistry (Robinson et al., 2018; Taniguchi et al., 2019), while temporal variabilities in groundwater / surface water interactions induce biogeochemical hot moments within the hyporheic zone (McClain et al. 2003; Boano et al. 2014; Lewandowski et al. 2019). The monitoring of groundwater fluxes at different depths during a pumping test would be also very useful to image flow variability and sub-surface heterogeneities (Pouladi et al. 2021b).

The temporal and spatial variability of groundwater fluxes depends on many natural or man-induced mechanisms which induce fluctuations in groundwater levels at different time scales (Freeze and Cherry 1979; Jiménez-Martínez et al. 2013). Short-lived fluctuations can typically be observed during the recharge of highly heterogeneous systems (Ghasemizadeh et al. 2012; Pouladi et al. 2021b) while diurnal variations can occur for instance as the result of evapotranspiration, atmospheric pressure effects or else tidal effects (Ataie-Ashtiani et al. 2001; Paepen et al. 2020; LeRoux et al. 2021). Groundwater recharge through infiltration (Freeze, 1974) and bank-storage effects near streams (Winter et al. 1998; Boano et al. 2013; Harvey and Gooseff 2015) can induce seasonal fluctuations in groundwater levels, while climate changes and many human activities, such as groundwater pumping, artificial recharge, agricultural irrigation and drainage or else geotechnical

drainage, induce short-term as well as long-term fluctuations of groundwater levels (Freeze and Cherry 1979; Hancock 2002; de Graaf et al. 2019).

Many approaches have been tested for monitoring and quantifying the temporal dynamic of groundwater fluxes in saturated porous media. Some of them, including isotopic tracers (Burnett et al. 2006; Garcia-Orellana et al. 2021) or the use of piezometers (Freeze & Cherry, 1979), only provide averaged values of fluxes over large spatial scales, which are not representative of their spatial variability induced by heterogeneities. In coastal environments, the use of geophysical methods was proposed to assess freshwater fluxes over a tidal cycle (Dimova et al. 2012; Folch et al. 2020) or seasonal variations in submarine groundwater discharge in the intertidal zone (Paepen et al. 2020). While such methods are suitable to investigate subsurface structures and heterogeneities (Binley et al. 2015; Brunner et al. 2017), they remain limited for continuous monitoring of groundwater fluxes due to relatively long data acquisition times. Specific methods based on tracer experiments, like the borehole dilution method (Drost et al. 1968; Pitrak et al. 2007) or the Finite Volume Point Dilution Method (Brouyère et al. 2008), also appear to be promising techniques for the continuous monitoring of groundwater fluxes (Jamin et al. 2015; Jamin and Brouyère 2018). However, their use provides a spatially-averaged value of fluxes over the well length, or over the volume investigated, and would require repeating point measurements at different depths to investigate the flow distribution.

Heat has also been efficiently used as tracer of groundwater fluxes in many contexts to study vertical fluxes and their temporal dynamics (Anderson 2005; Rau et al. 2014; Kurylyk et al. 2019). Passive heat tracing experiments rely on the continuous monitoring of natural temperature variations within the saturated subsurface during several days, weeks or months. Even if the use of passive tracer experiments allows quantifying groundwater flow variations over time, analytical and numerical models commonly used to interpret temperature time series generally assume constant daily fluxes (Hatch et al. 2006; Keery et al. 2007; Constantz 2008; Briggs et al. 2012). This means that passive experiments only provide an averaged daily value of groundwater fluxes and are not suited for characterizing groundwater fluxes variations occurring at shorter time scale. Very recent developments discussed the feasibility of monitoring transient flows from temperature-depth profiles (Lin et al. 2022). However, such approach does not provide fluxes spatial distributions and estimates are dependent of natural temperature variations, which limits the applicability of the method in many environments.

The development of Fiber Optic Distributed Temperature Sensing (FO-DTS) technology, providing continuous temperature data along fiber optic cables at high spatial and temporal resolution, largely enhanced the use of heat as groundwater tracer for environmental applications (Selker et al. 2006; Tyler et al. 2009; Shanafield et al. 2018). Its use can be well suited to characterize diurnal temporal flow variations, as demonstrated by Henderson et al. (2009) but also to qualitatively study seasonal and temporal fluctuations of groundwater discharge into surface water (Slater et al. 2010; Sebok et al. 2013; Matheswaran et al. 2014). However, the approach does not allow characterizing short-scale variations of groundwater fluxes and quantifying groundwater fluxes through passive DTS measurements remains difficult and uncertain (Le Lay et al. 2019; Simon et al. 2022).

Recent developments have shown that active-DTS performs very well for investigating the spatial distribution of groundwater fluxes over a large range of values at an unprecedented high spatial resolution (Simon et al. 2021). Active-DTS methods consist of continuously recording the temperature changes induced by a heat source applied along a Fiber Optic (FO) cable. The difference of temperature measured between a heated and a non-heated FO cable directly depends on the flow rate (Read et al. 2014; Bakker et al. 2015; Sayde et al. 2015; Bense et al. 2016; Simon et al. 2021).

Since the temperature increase measured during heat injection directly depends on groundwater fluxes, any change in groundwater flow occurring during the heating period should result in a change in temperature variation. Therefore, the method should be well suited for continuously monitoring groundwater flow variations. This assumption is supported by the fact that Sayde et al. (2015) used actively heated fiber optics for continuously monitoring wind speed changes over time and therefore demonstrated that the temperature elevation measured during heating experiments is sensitive to wind speed variations.

Few studies investigated the interest of repeating active-DTS measurements under different hydrological conditions to study thermal properties changes or groundwater fluxes variability (Abesser et al. 2020; Munn et al. 2020), but the approach has never been used to continuously monitor groundwater flow variations with time. All previous applications of active-DTS have been performed under steady-state flow conditions (during the heating period).

In this study, we therefore propose to investigate the potential of active-DTS measurements for continuously monitoring groundwater fluxes changes over time in fully saturated media. The main objective is to verify if the temperature evolution measured during heating injection is sensitive to groundwater flow variations (transient flow conditions). An increase of groundwater flux should lead to a decrease of temperature (groundwater flow dissipating more efficiently the artificial heat injected) and vice versa. The question of the shape/duration of the flow change will also be investigated. We aim to understand how instantaneous, progressive and periodic flow changes will affect the thermal response. For doing so, we first rely on simple theoretical developments that are complemented by numerical simulations and sandbox experiments. Numerical modeling is used to validate the theoretical developments and to simulate the effect of flow fluctuations on the thermal response in various conditions. Then, we rely on an experimental validation by achieving active-DTS measurements in a sandbox. By associating theoretical developments, numerical modeling and laboratory experiments, we aim to verify the potentiality and the limitations of active-DTS experiments for monitoring groundwater flows at high spatial resolution.

2. Material & Methods

2.1. Mathematical and theoretical formulation

2.1.1. Background

Among active-DTS experiments, our interest in this study is a recently-used setup which consists of electrically heating a FO cable through its steel armoring while continuously monitoring the elevation in temperature all along the heated section using the FO inside the cable. In such configuration, a single FO cable is used as a heat source and as a temperature measurement tool (Bense et al., 2016; Read et al., 2014; F. Selker & Selker, 2018; Simon et al., 2021). In this case, as recently shown by Simon et al. (2021) and del Val et al. (2021) and illustrated in Figure 1, the total temperature increase ΔT is the result of two terms:

$$\Delta T = \Delta T_{FO} + \Delta T_{PM} \quad (1)$$

ΔT_{FO} is the result of the heat storage and heat conduction occurring within the FO cable. The electrical heating induces indeed a relatively large increase of temperature during the early period of heating ($t < t_c$). Note that t_c corresponds to the limit beyond which the temperature elevation is no

longer affected by the heat conduction and storage through the FO cable (ΔT_{FO} is maximum and constant for t > t_c). As soon as the heat produced reaches the surrounding material, the temperature increase is controlled by heat conduction and advection occurring through the porous media surrounding the FO cable, which both dissipate a part of the heat produced. The associated temperature rise (ΔT_{PM}) depends on both thermal conductivity and Darcy velocity. For sufficient long times, heat conduction and advection may fully dissipate the heat produced, leading to the temperature stabilization (ΔT_f). The higher the groundwater flux, the lower the temperature of stabilization and the faster steady conditions are reached (Figure 1). If q=0 (no groundwater flow), the temperature keeps increasing gradually and never stabilizes (Carslaw and Jaeger, 1959; Diao et al. 2004; Simon et al. 2021).

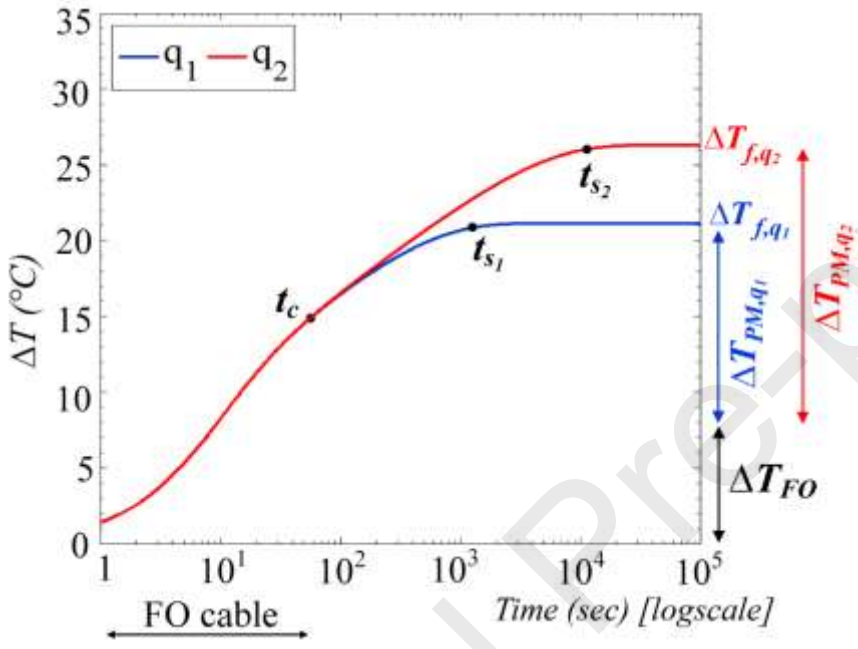

Figure 1: For similar sediments thermal properties conditions, the temperature increase depends on groundwater flow. Red and blue lines correspond to temperature elevations observed for different values of groundwater fluxes q_1 (blue line) and q_2 (red line) (with $q_1 > q_2$).

ΔT_{FO} depends on the heating rate power and on the thermal properties of the heating cable and is independent of both the thermal properties of the material and the flow conditions. As validated by Simon et al. (2021), the evolution of ΔT_{PM} can be modelled over time using the Moving Instantaneous Line Source (MILS) model, initially developed by Carslaw and Jaeger (1959). By considering an initial thermal equilibrium T_0, the thermal response ΔT_{PM} ($\Delta T = T - T_0$) along the line source is given in *x*-*y* direction by:

$$\Delta T_{PM}(x,y) = \frac{Q}{4\pi\lambda} exp\left[\frac{q\,x}{2D_t}\frac{\rho_w c_w}{\rho c}\right] \int_{\frac{x^2+y^2}{4tD_t}}^{\infty} \exp\left[-\Psi - \left(\frac{x^2+y^2}{D_t}\right)\frac{q^2}{16D_t\Psi}\frac{\rho_w {}' c_w {}'}{\rho {}' c^2}\right]\frac{d\Psi}{\Psi} \qquad (2)$$

With q the uniform and constant groundwater flux in x-direction (or specific discharge) (m.s^{-1}) and Q the constant and uniform heating rate power (W.m^{-1}). The coordinates x and y correspond to the distance from the heat source, located at $x = 0$ and $y = 0$ and Ψ is a change of variable. ρc is the volumetric heat capacity of the rock-fluid matrix (J.m^{-3}.K^{-1}) and $\rho_w c_w$ the volumetric heat capacity of

165 water ($J.m^{-3}.K^{-1}$). The parameter D_t is the thermal diffusivity coefficient ($m^2.s^{-1}$) and corresponds to
166 the ratio between λ, the bulk thermal conductivity ($W.m^{-1}.K^{-1}$), and ρc.

167 Equation 2 can be simplified for $t \rightarrow \infty$ using the Bessel function of second kind and order
168 zero K_0 (Diao et al. 2004; des Tombe et al. 2019):

$$\Delta T_f = \frac{Q}{2\pi\,\lambda}\, exp\left[\frac{q\ x}{2D_t}\ \frac{\rho_w c_w}{\rho c}\right] K_0\left(\frac{rq}{2D_t}\ \frac{\rho_w c_w}{\rho c}\right) \quad (3)$$

169 where ΔT_f is the temperature stabilization. Note that this solution can be used only when temperature
170 stabilization is reached, for steady-state hydraulic and thermal conditions.

171 **2.1.2. Theoretical Formulation for Transient Hydraulic conditions**

172 As illustrated in Figure 1, the temperature increases ΔT_{q_1} and ΔT_{q_2}, respectively associated to
173 groundwater fluxes equals to q_1 and q_2, are given for any $t > t_c$ by:

$$\Delta T_{q_1}(t) = \Delta T_{FO} + \Delta T_{PM,q_1}(t) \quad (4)$$

$$\Delta T_{q_2}(t) = \Delta T_{FO} + \Delta T_{PM,q_2}(t) \quad (5)$$

174 $\Delta T_{PM,q_1}$ and $\Delta T_{PM,q_2}$ correspond to temperature rises associated to heat conduction and advection
175 occurring through the porous media, for groundwater fluxes respectively equals to q_1 and q_2 and can
176 be calculated using the analytical form (Equation 2).

177 For thermal steady-state conditions, ΔT_{PM} can be modelled using Equation 3, which means that
178 Equations 4 and 5 become for late time:

$$\Delta T_{q_1}(t) = \Delta T_{FO} + \Delta T_{f,q_1} \quad (4a)$$

$$\Delta T_{q_2}(t) = \Delta T_{FO} + \Delta T_{f,q_2} \quad (5a)$$

179 The heat conduction through the FO cable, inducing the temperature increase ΔT_{FO}, only occurs for
180 short time and is independent of groundwater flux. Thus, for late time, we obtain by subtracting
181 Equations 4a and 5a:

$$\Delta T_{q_2}(t) - \Delta T_{q_1}(t) = \Delta T_{f,q_2} - \Delta T_{f,q_1} \quad (6)$$

182 Equation 6 means that the difference of temperature stabilization for q_1 and for q_2 can easily
183 be modelled using Equation 2. It suggests that, for a groundwater flux change from q_1 to q_2 and for
184 long enough steady-state conditions, the temperature stabilizes depending on q_2 and that the
185 temperature increase or decrease after the flow change directly equals to the difference between the

temperature of stabilization observed for q_1 (under stationary flow conditions) and the temperature of stabilization observed for q_2 (under stationary flow conditions).

Then, the temperature evolution in response to groundwater flow variations can be seen as the superposition of different hydrological conditions, each one being described by the solution calculated for a given flow. Thus, in theory, the superposition principle could be applied to interpret temperature in varying groundwater flow conditions. This means that the temperature following a sharp or sudden change q_1 to q_2 should be given (for any $t > t_c$) by:

$$\Delta T_{q_{1\to q2}}(t) = \Delta T_{q_1}(t) - \Delta T_{q_1}(t') + \Delta T_{q_2}(t') \quad (7)$$

With $t'=t-t_1$, t_1 being the time for which the change of groundwater flow occurs. Combining equation 7 with equations 4 and 5 leads to:

$$\Delta T_{q_{1\to q2}}(t) = \Delta T_{FO} + \Delta T_{PM,q_1}(t) - \Delta T_{PM,q_1}(t') + \Delta T_{PM,q_2}(t') \quad (8)$$

If we assume that t_1 is larger than the time required to reach temperature stabilization for $q=q_1$, equation 8 becomes :

$$\Delta T_{q_{1\to q2}}(t) = \Delta T_{FO} + \Delta T_{f,q_1} - \Delta T_{PM,q_1}(t') + \Delta T_{PM,q_2}(t') \quad (9)$$

In other words, Equation 9 means that the evolution of the temperature after the change from q_1 to q_2 could be obtained by adding, to the temperature recorded at t_1, the difference of the temperature elevation associated to heat conduction and advection occurring through the porous media for groundwater fluxes respectively equals to q_1 and q_2. Note that temperature should increase if $q_1 > q_2$ and decrease for $q_1 < q_2$. If t_1 is smaller than the time required to reach temperature stabilization, Equation 8 should be used instead of Equation 7, but the same principle should apply and the change of flow should lead to a temperature change related to the difference: $-\Delta T_{PM,q_1}(t') + \Delta T_{PM,q_2}(t')$.

Thus, if we suppose a groundwater flux change from q_1 to q_2 occurring at $t=t_1$, we expect the following implications from equations 8 and 9 :

1) at late times after flow change ($t >> t_1$), the temperature should stabilize depending on the last flux imposed (q_2) and independently of previous fluxes conditions and temperature variations (Equation 4b). Consequently, any temperature stabilization recorded during heating periods should reflect steady flow conditions and could be used to quantify associated groundwater fluxes.

2) The temperature evolution after any flow change should be modeled by applying the superposition principle (Equation8 or 9). This involves that, besides the temperature stabilization at late times, the temperature evolution in time could also be possibly used to quantify q_2.

2.1.3. Objectives of the study

To verify the previous developments, we rely on experiments conducted in a sandbox where the flow rate can be controlled and changed during active-DTS measurements. The temperature evolution is continuously recorded in response to successive flow rates to verify if the analytical

solution (MILS) can actually be used to model temperature changes over time and to quantify groundwater flow changes.

The question of the shape/duration of the flow change should also be addressed. We expect that the thermal response to flow change would be different in case of sharp and instantaneous flow change or in case of progressive flow change. In both cases, we want to investigate the time required to reach a new thermal steady regime after flow change. Theoretically, the stabilization time should depend on q_2, since the smaller the flux, the greater the time necessary to reach temperature stabilization (Simon et al. 2021). Likewise, we aim to investigate the feasibility of monitoring periodic groundwater fluxes, as observed in coastal aquifers for instance. In theory, if temperature evolution is sensitive to water flow changes, we expect to observe a periodic temperature signal while flow changes periodically. Thus, for progressive or periodic flow changes, a critical point will be to define if temperature changes occur simultaneously to flow variations and therefore if the approach allows continuous and real-time monitoring of flow variations.

With this in mind, since flow changes that can be applied in the sandbox are quite limited, we rely on numerical simulations to simulate active-DTS measurements conducted under transient flow conditions. Thermal responses to different scenarios of flow variations are modelled (instantaneous, progressive and periodic flow changes) to investigate the effect of flow changes rate on temperature evolution.

2.2. Numerical modeling

2.2.1. Numerical Model

To simulate heat transfer occurring in a porous media during active-DTS measurements and to assess the effect of flow changes, we use a 2D domain numerical model of flow and heat transport implemented in COMSOL Multiphysics®. The Multiphysics software COMSOL solves heat and flow transfers equations using finite element methods. This model includes an explicit representation of FO cables used for field experiments (BRUSens cables LLK-BSTE 85°C) consisting of a steel core (1.13 mm radius; λ = 13.4 $W.m^{-1}.K^{-1}$) and a plastic jacket (1.925 mm radius; λ = 0.245 $W.m^{-1}.K^{-1}$). A heat source term is added in the steel core and simulations are run by fixing the electrical power input injected along the FO cable at 35 $W.m^{-1}$. The domain is modeled as a rectangle whose size is fixed at 3 x 1 m and the heat source is applied at 1 m of the laminar inflow boundary condition, the flow being lengthwise. We ensured that the heat produced does not reach the domain boundaries for any flow conditions tested in this study. The thermal conductivity of the porous media is fixed at λ = 1.1 $W.m^{-1}.K^{-1}$ and its volumetric heat capacity at $\rho c = 3x10^6$ $J.m^{-3}.K^{-1}$.

This model has already been used in a previous study to understand the thermal processes controlling the temperature increase measured along a heated FO (Simon et al. 2021). Its use allowed validating the data interpretation framework presented in the section 2.1.1 (“Background”) and the use of the MILS model (Equation 2) to estimate groundwater fluxes. However, the model has, up to now, always been used in steady-state fluid flow conditions. Here, simulations were performed by considering transient flow conditions during heating periods.

2.2.2. Sharp and progressive groundwater flow changes

Firstly, sharp or progressive groundwater flow variations (from q_1 to q_2) have been simulated, as shown in Figure 2. The temperature elevation is first simulated considering steady-state fluid flow conditions by applying a constant and uniform flow q_1. After several hours of heating, a sharp or progressive flow change is simulated to reach a lower flow rate q_2. In order to assess the effect of the flow change rate and of the flow change intensity on temperature variations, different scenarios are

considered as detailed in Figure 2. Case 1 simulates a groundwater flow decrease from q_1 = 3.6x10^{-5} m.s^{-1} to q_2 = 1.2x10^{-5} m.s^{-1}, while case 2 simulates a groundwater flow decrease from q_1 = 3.6x10^{-5} m.s^{-1} to q_2 = 3.2x10^{-5} m.s^{-1}. In both cases, the change of flow is occurring three hours after the start of the heat injection, once temperature stabilisation has already been reached for flow q_1. For each case, the applied flow change from q_1 to q_2 is either instantaneous and so very sharp (blue line) or smoothed and progressive along time with transition periods varying between 30 minutes and 8 hours. With these two cases, modeling focuses on assessing the effect of the difference between q_1 and q_2 on temperature evolutions and on comparing the flow change rate with the temperature change rate.

Besides, it has been proven in steady-state flow conditions that a gradual and continuous temperature rise during heating period without temperature stabilization at late times occurs in case of no groundwater flux (Diao et al. 2004; Simon et al. 2021). Thus, after a change from flow to no-flow conditions, it can be expected that, the temperature evolution shows a similar behaviour and that a continual temperature rise would be observed under no-flow conditions. To address this point, a complementary simulation is run to simulate a change from flow conditions q_1 = 1.2x10^{-5} m.s^{-1} to no-flow conditions q_2 = 0 m.s^{-1}.

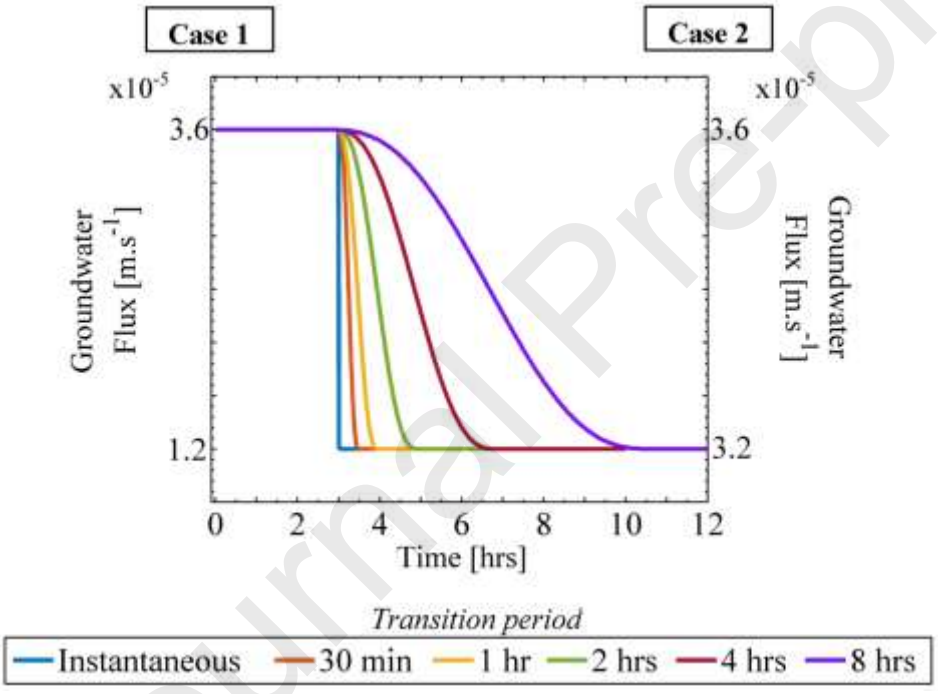

Figure 2.. Illustration of groundwater flow changes simulated in Case 1 and Case 2.

2.2.3. Periodic hydraulic flow variations

The second set of simulations consists of simulating periodic groundwater flow variations. For these simulations, the period of the sine signal is set to 12 h (1/43200 Hz) approximating the period of tidal cycles (≈ 12.4 h). For the first case with sine variations, the amplitude of the signal is 2.4x10^{-5} m.s^{-1} and flow vary between 1.2x10^{-5} and 3.6x10^{-5} m.s^{-1} (Figure 6a). For the second one, a smaller amplitude is considered (8x10^{-6} m.s^{-1}) with fluxes varying between 2.8x10^{-5} and 3.6x10^{-5} m.s^{-1} (Figure 6b).

2.3. Laboratory tests

Active-DTS measurements were carried out during sandbox laboratory experiments. The experimental setup consisted of burying a heatable FO cable in a sandbox in which flow rates can be well-controlled. The sandbox is a 0.576 m^3 PVC tank open at the top (1.6 m long; 1.2 m width and 0.3 m height) and filled with 0.4-1.3 mm diameter quartz sand (Figure 3a). The height of water in reservoirs on two sides of the sandbox can be manually adjusted to control the hydraulic gradient and thus the water flow through the sand. The flow through the sandbox is considered homogeneous and the average hydraulic conductivity is estimated equal to $3x10^{-3}$ $m.s^{-1}$. The FO cable buried in the sandbox is a 3.8-mm-diameter cable containing 4 multimode 50/125-µm fibers (BruSens cable; reference LLK-BSTE 85°C). A 7 m-section of this cable was electrically isolated and connected to an electrical allowing the injection of electricity from a power controller. DTS measurements were carried out with a Silixa Ultima S DTS unit used in double-ended configuration (van de Giesen et al. 2012) and reporting temperature every 12.5 cm at a-20 seconds sampling interval (10 seconds per channel). Cold and warm baths were used to calibrate temperature measurements (Figure 3a). The relative uncertainty of measurements was estimated to 0.03°C while absolute uncertainty was estimated equal to 0.15°C. The effective spatial resolution of the unit was experimentally estimated during heating periods to be between 51 and 67 cm (Simon et al., 2020). A succession of active-DTS measurements was already conducted under steady-state flow conditions using this setup and associated measurements have already been the subject of two precedent studies (Simon et al. 2020; Simon et al. 2021).

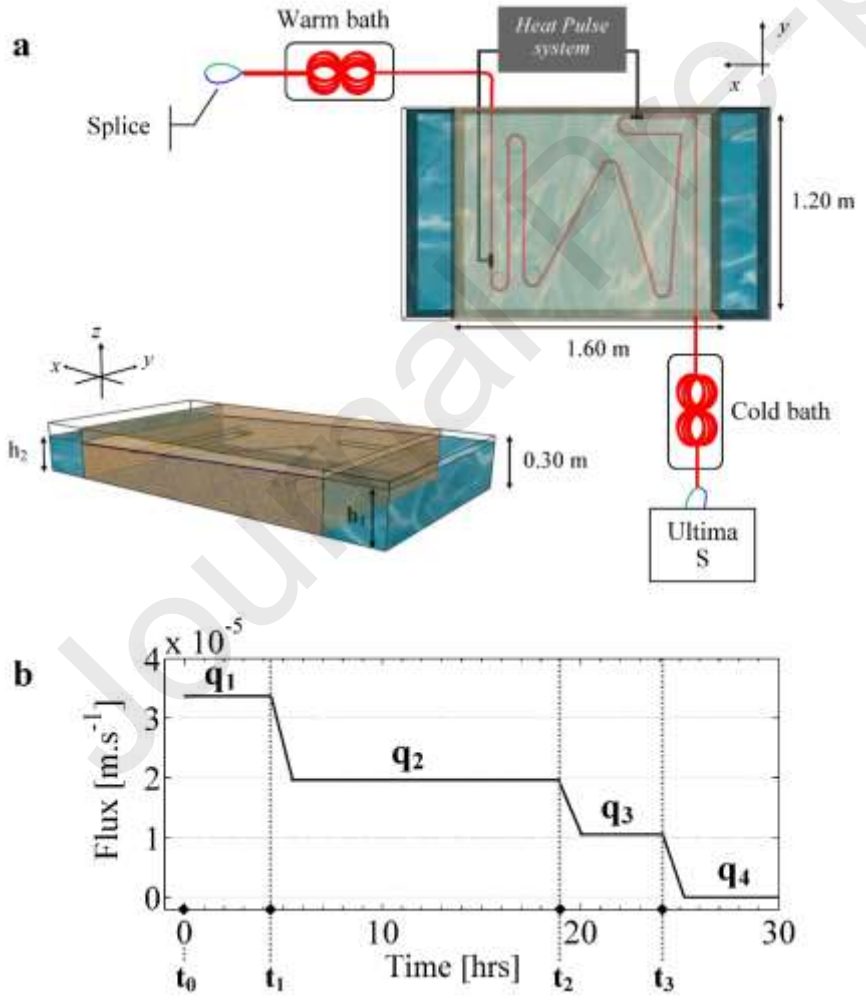

Figure 3. a. Experimental Setup of the sandbox experiment (modified from Simon et al. 2020); b. Steps of water fluxes imposed through the sandbox over the heating period

For this study, the heatable section of the FO cable was continuously energized for 29 hours using a Silixa Heat Pulse Control System, delivering a well-controlled power intensity of 15 $W.m^{-1}$ along the heated section. For the first 4-hrs of the heat injection, the flux was held constant and estimated at $3.37x10^{-5}$ $m.s^{-1}$ (Figure **Error! Reference source not found.**b). Then, a three-step decrease of the groundwater flow was applied until no-flow condition ($q = 0$) was reached at the end of the experiment. The water fluxes associated to each step are noted q_1, q_2, q_3 and q_4. In practice, the flow through the sandbox is changed by manually decreasing the height of water in the inlet reservoir, which induces a decrease of the hydraulic gradient and thus of the water flux. It involves for each change a period of transient-flow conditions before a new steady-state condition is reached. The duration of these transient-flow conditions periods is difficult to assess since hydraulic heads changes are not monitored. However, from the observations made during the experiment, we consider steady-state flow is reached in approximatively 30 minutes after flow changes, which is consistent with the permeability estimated.

3. Results

3.1. Numerical modeling

3.1.1. Sharp and progressive flow changes

Figure 4 presents temperature transients modelled for Case 1 (Fig. a and b) and for Case 2 (Fig. c and d). For the first case, the heat injection at t=0 induces a sharp increase of temperature (Fig. 4a). The temperature stabilizes rapidly (in around 25 min) at 17.42°C depending on experimental conditions (thermal properties of FO cable, power injected), on thermal properties of the porous media but especially on flux ($q_1 = 3.6x10^{-5}$ $m.s^{-1}$). After three hours of heating, a groundwater flow decrease is modelled to reach $q_2 = 1.2x10^{-5}$ $m.s^{-1}$. It induces an increase of temperature, which is in perfect agreement with expectations: for lower groundwater flow, heat produced is less dissipated by advection leading to a temperature increase. In this case, independently of the duration of the hydraulic transition period, the temperature increases and stabilizes at 21.26°C, which corresponds to the temperature stabilization predicted by the model considering steady flow conditions q_2 for the whole heating period (dotted grey line). Thus, the temperature stabilization after the flow change clearly depends on the groundwater flow q_2.

However, the duration of the hydraulic transition period also affects the temperature variations and the duration of thermal transition period, as detailed in Fig. 4b which shows temperature evolutions modelled after the start of the flow change (ΔT is calculated here as the difference between the temperature simulated for any $t > 3$ h and the temperature at $t = 3$ h, corresponding to the stabilization temperature for q_1). For an instantaneous and sharp flow change (blue line), the temperature elevation does not instantaneously stabilize but progressively increases up to reaching stabilization (approximately 3 hours after the flow change). In this case, the superposition principle can be used (Equation 7) to reproduce the temperature change observed after the flow change (Results are not shown here to not overload the Figure).

For simulations considering smoothed transition periods of 30 min (orange line), 1 h (yellow line), 2 h (green line) and 4 h (brown line), results show that reaching steady temperature conditions is longer than reaching steady flow conditions. Temperature and flow changes are not simultaneous and the temperature response is delayed. However, although difficult to observe in Figure 4b because of the logscale that compress the late times, when the transition period increases, the delay between the temperature stabilization and the flow stabilization decreases. Thus, if the hydraulic transition period lasts 4 hours, the temperature stabilization is reached in 4h45min. For longer transition periods (see for instance purple line corresponding to an 8-hrs transition period), the temperature stabilization is reached at the same time as the flow steady conditions, meaning that temperature

changes are occurring at the same rate as flow changes. Subsequently, if flow changes are smoothed enough, it becomes possible to monitor flow changes in real time. For these cases, using the simplest version of the superposition principle (Equation 7) does not allow reproducing the thermal response observed in response to flow change. However, regardless of the shape and duration of the transient flow stage, the temperature systematically stabilizes depending on the value of q_2, which means that the value of the temperature stabilization can be used to estimate q_2 using the MILS model (Equation 2) or its simplified version (Equation 3).

Fig. 4c and d present thermal response to flow change from $q_1 = 3.6 \times 10^{-5}$ m.s^{-1} to $q_2 = 3.2 \times 10^{-5}$ m.s^{-1}. Temperature responses for the three first hours are similar to thermal responses presented in Case 1 (identical steady flow conditions). Then, the flow change induces an increase of temperature but the temperature stabilization for this case is lower than case 1 (17.81°C) in agreement with a greater value of q_2. Actually, as observed for Case 1, the temperature stabilizes according to the temperature value expected for q_2 (dotted grey line). This confirms that if steady flow conditions are long enough after the flow change, thermal steady conditions (temperature stabilization) are reached independently of earlier flow conditions. However, the time required to reach the thermal stabilization depends on the rate of flow variations. Thus, the temperature stabilizes faster for case 2 than for case 1. For an instantaneous flow change (blue line), temperature approximately stabilizes 18 min after the start of flow change (against 3 h for Case 1). Likewise, as soon as the transition period exceeds 1 h, the temperature stabilization is reached at the same time as the flow steady conditions. Thus, our results show that the duration of the transient temperature variations depends on the value of q_2 but also on the intensity of flow variation (the difference between q_1 and q_2).

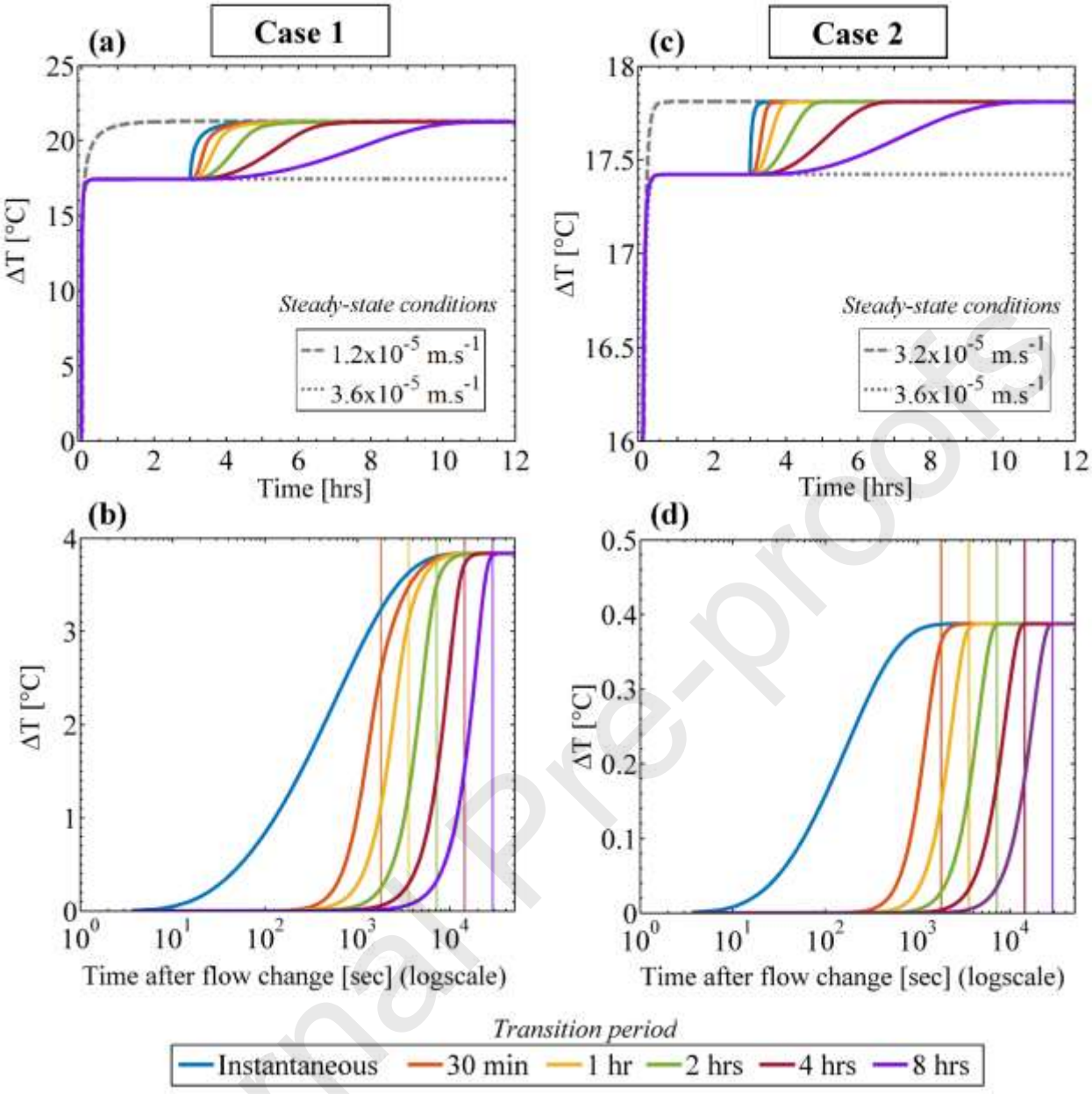

Figure 4. a. Temperature evolutions modelled for Case 1 considering a flow change from q_1 = 3.6x10^{-5} m.s^{-1} to q_2 = 1.2x10^{-5} m.s^{-1} three hours after the start of the heating period. Colored lines correspond to the different durations of transient flow conditions tested. Grey lines correspond to temperature evolutions predicted by considering steady flow conditions (respectively q_1 and q_2) for the whole heating period. b. ΔT calculated after change in flow conditions considering the difference between the temperature simulated for any t > 3 h and the temperature at t = 3hrs. Vertical colored lines correspond to the duration of each hydraulic transition period tested. Likewise, figures c and d present results for Case 2 considering a flow change from q_1 = 3.6x10^{-5} m.s^{-1} to q_2 = 3.2x10^{-5} m.s^{-1} occurring three hours after the start of the heating period.

In complement to previous results, simulations were run to simulate an instantaneous change applied at t = 3hrs from flow conditions q_1 = 1.2x10^{-5} m.s^{-1} to no-flow conditions q_2 = 0 m.s^{-1}. In this case (Figure 5), the temperature rises progressively and almost 24 hrs are required so that the temperature elevation reaches the temperature curve modelled by considering no-flow conditions for the whole heating period. The absence of groundwater flow after the change means that heat dissipation occurs only through heat conduction, which involves slow and less efficient heat

transfers. Although no temperature stabilization occurs for late times, the superposition principle (Equation 8) can efficiently be used to reproduce the temperature elevation observed after the flow change.

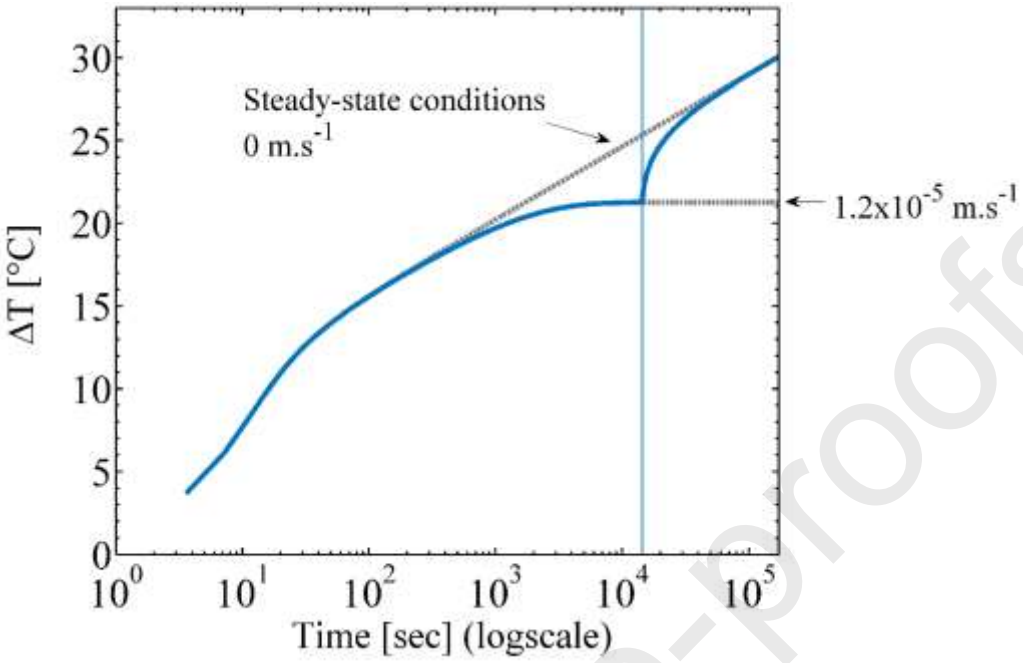

Figure 5. Blue line corresponds to temperature evolution modelled by considering a flow change from q_1 = 1.2x10^{-5} m.s^{-1} to no-flow conditions occurring three hours after the start of the heating period. Dotted grey lines correspond to temperature evolutions modelled

3.1.2. Periodic groundwater flow variations

Figures 6a and b present temperature responses modelled in response to periodic flow changes occurring during the heating period. In this first case, the period of the sine signal is set to 12h with fluxes varying between 1.2x10^{-5} and 3.6x10^{-5} m.s^{-1} (blue line in Fig. 6a). Brown line corresponds to the associated temperature variations (heating period starting at t=0). Temperature oscillates between 17.42 and 21.18°C in response to flow changes (an increase of flux inducing a temperature decrease and vice versa). Interestingly, a delay in time (≈20 min) can be observed between maximum temperature peaks and minimal fluxes (Fig. 6a). On the opposite, minimum temperature peaks and maximal fluxes are perfectly synchronized. Actually, as shown in Figure 6b, while groundwater flow is maximal (and therefore the temperature elevation minimal), the temperature elevation reaches 17.42°C, which corresponds to the stabilization temperature of the model considering steady flow conditions and q=3.6x10^{-5} m.s^{-1}. However, while groundwater flow is minimal (and therefore the temperature elevation maximal), the temperature elevation only reaches 21.18°C, which is slightly less than the expected temperature (the stabilization temperature of the model considering steady flow conditions and q=1.2x10^{-5} m.s^{-1} being 21.3°C).

Then, the amplitude of the sine signal was decreased with fluxes varying between 2.8x10^{-5} and 3.6x10^{-5} m.s^{-1}. Associated results are presented in Figures 6c and d. In this case, temperature oscillated between 17.42 and 18.26°C. Contrary to previous flow conditions, peaks in temperature are perfectly synchronized with peaks in fluxes (Fig 6c). A shown in Fig 6d, the minimum and maximum temperatures reached are in perfect agreement with stabilization temperatures obtained while considering steady flow conditions of 2.8x10^{-5} and 3.6x10^{-5} m.s^{-1}. These results seem very promising concerning the applications of active-DTS measurements under transient flow conditions.

It suggests that while flow variations are smoothed, temperature elevation changes occur simultaneously to flow variations and can therefore be used to continuously monitor and characterize transient flows. These results suggest that the feasibility of monitoring fluxes depends on the values of q_1 and q_2 and on the difference between them.

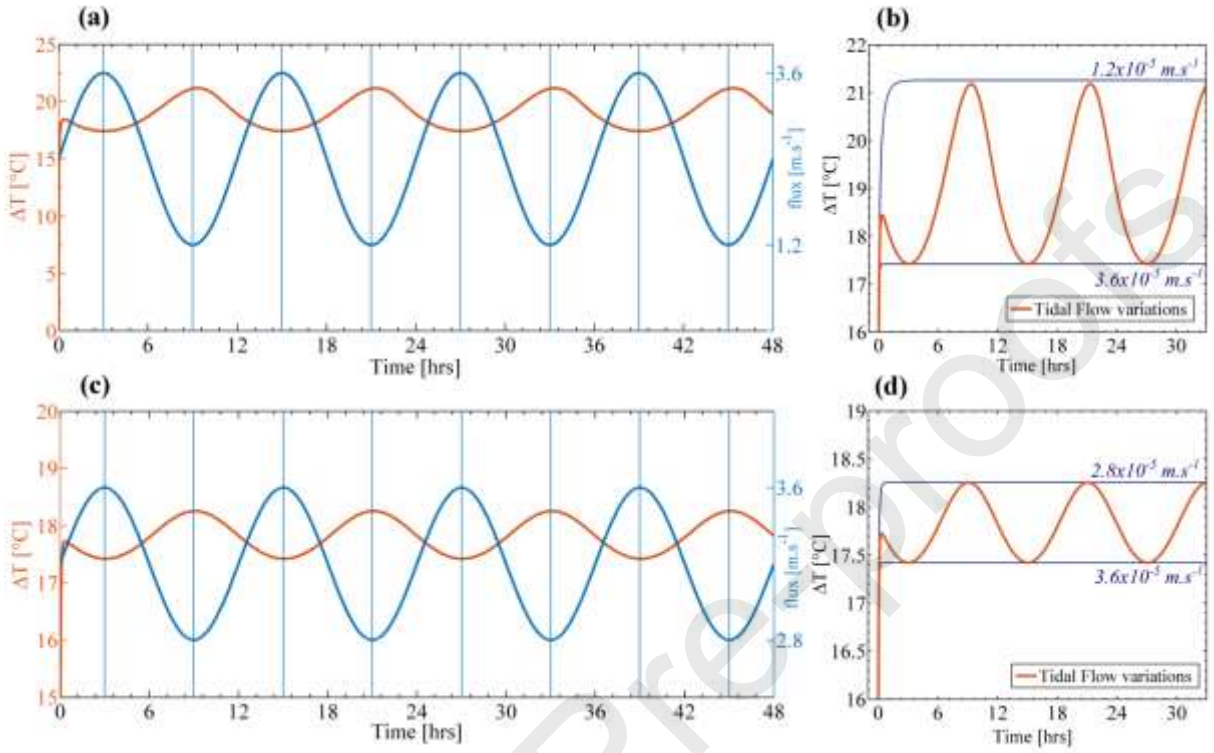

Figure 6. Results of simulations considering periodic groundwater flow variations. a. Temperature evolution (brown line) modelled in response to groundwater flow changes (blue line). The period of the sine signal is set to 12h with fluxes varying between $1.2x10^{-5}$ and $3.6x10^{-5}$ $m.s^{-1}$. Vertical lines indicate times of maximal and minimal groundwater fluxes. b. Temperature evolutions considering either periodic groundwater flow variations (brown line) or steady flow conditions (blue lines). Likewise, figures c and d present results of simulations considering periodic groundwater flow variations varying between $2.8x10^{-5}$ and $3.6x10^{-5}$ $m.s^{-1}$.

3.2. Laboratory tests

Figure 7 shows the temperature increase ΔT measured along the FO cable in response to heat injection (red line). Note that the temperature variations presented here were recorded along a section of the cable positioned perpendicular to the main flow direction. At $t = t_0 = 0$, the electrical power is switched on. The start of the heating period is associated to a rapid and sharp temperature change that reaches 8.8 °C in 2 minutes. After 16 minutes of heating, the temperature stabilizes around 10 °C, meaning that the thermal steady-state is reached. At $t = t_1$, while the flow is decreased from q_1 to q_2, a significant temperature rise is measured. The temperature first increases rapidly before stabilizing around 10.5 °C. Then, at $t = t_2$, while the flow is decreased from q_2 to q_3, another significant temperature rise is observed. The temperature increases up to stabilizing at 10.9 °C 1h50 after the flow change. Finally, at $t = t_4$, the water flow is turned off (no-flow conditions), which induces a new temperature increase.

3.2.1. Modeling the temperature stabilization

The first three flow changes applied during the heating period induced a transient thermal stage followed by a temperature stabilization stage at higher temperature. Following Equation 5a, the temperature theoretically stabilizes at late times according to flow conditions occurring after each flow stage. Thus, it should be possible to model the temperature of stabilization observed for each stage using the analytical model considering associated groundwater fluxes. This is presented in Figure 7, which compares the temperature increase measured during the heating period (red curve) with modelled curves (grey lines), simulated following Equation 2. Note that Equation 3 can also be used to directly match temperature stabilization values with flow estimates. The value of ΔT_{FO} is set at 7.09 °C in accordance with the results of Simon et al. (2021) and with the heating rate power (15 $W.m^{-1}$). Each curve is simulated by considering a specific value of flux (q_1, q_2, q_3 or q_4) corresponding to the different steps of water flow imposed through the sandbox over the heating period, indicated on the top of the Figure.

As expected, for the first flow-step, from t_0 to t_1, the thermal response can be very well reproduced using the MILS model, as the flow is constant during this period. The RMSE between modelled and measured data from t_0 to t_1 is 0.06 °C. After the first flow change applied at $t = t_1$, the measured temperature progressively increases and stabilizes at the temperature stabilization predicted by the model considering q_2. The RMSE between modelled and measured data during the associated temperature stabilization stage is 0.06 °C. This result confirms that, during heating periods, the temperature of stabilization exclusively depends on the effective groundwater flux at the time of the steady-state period and not on fluxes variations that have occurred in earlier times.

For the third stage, the temperature of stabilization reached for the third flow-step (q_3) also corresponds to the temperature of stabilization expected under flow-conditions such as $q = q_3$, although the experimental curve matches not as well with the modelled curve considering q_3 (the associated RMSE is 0.11 °C). In this case, as discussed further, this slight difference between modelled and measured data is due to the fact that the temperature stabilization is not fully reached. A longer period would have been required before applying another flow change to be able to perfectly model the temperature stabilization. When the last flow change is applied at $t = t_3$ imposing no-flow conditions in the sandbox, the measured temperature starts increasing. However, contrary to the previous steps, a significant difference is observed between the experimental curve and the modelled one considering q_4, even after a few additional hours of heating.

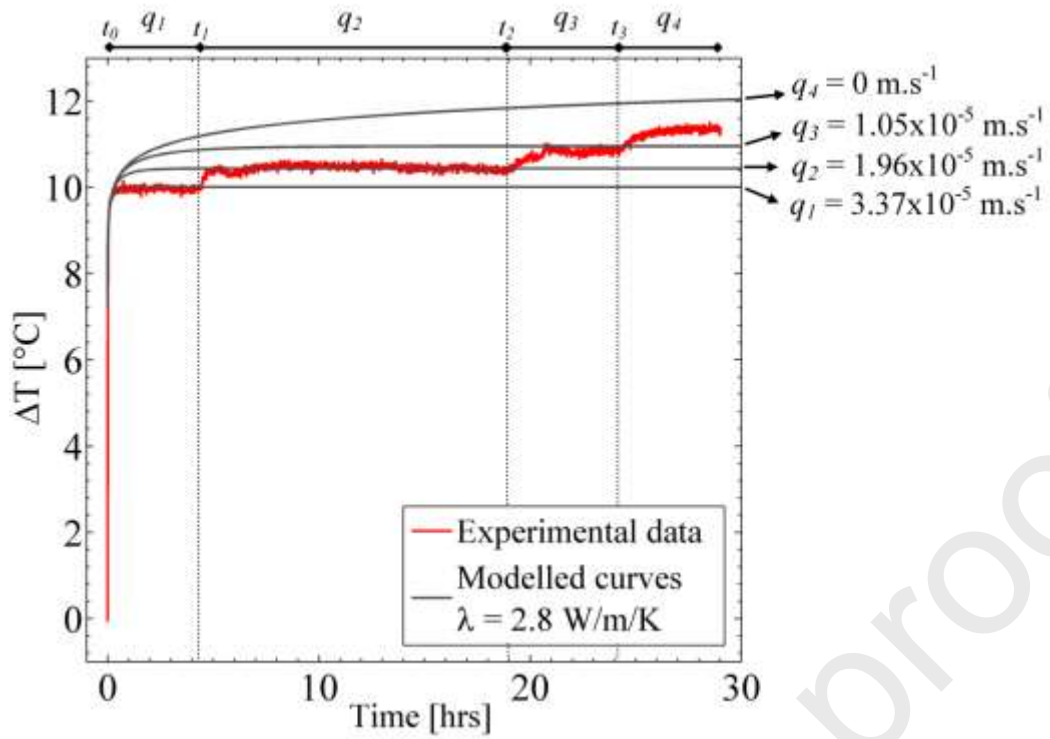

Figure 7. Comparison between the measured temperature increase (red line) and four curves modelled for different groundwater flux *q* under steady-flow conditions (black lines). Each of these curves is simulated using the MILS model (Equation 2) considering a specific value of flux (q_1, q_2, q_3 or q_4) corresponding to the different steps of water flow imposed through the sandbox over the heating period, indicated on the top of the Figure.

3.2.2. Modeling the real-time temperature increase

Theoretically, any instantaneous variation in the groundwater flow should induce a change in the temperature evolution which could be modelled using the superposition principle as described in Equation 8. This principle was used to reproduce the temperature evolution measured in the sandbox during the heating period. Figure 8 presents the step-by-step reproduction of the measured temperature increase considering each flow change applied over the heating period. Note that only the temperature variations induced by heat transfer through the porous ΔT_{PM}, calculated as $\Delta T_{PM} = \Delta T - \Delta T_{FO}$, are presented here. In each plot, the red line corresponds to the measured temperature increase and the black line to the modelled temperature increase established by considering flow variations applied over the heating period. For each case, blue line corresponds to the temperature increases that would have been observed if steady-flow conditions would have been applied during the whole heating period. For instance, in Figure 8b, the blue line called $\Delta T_{PM,q2}$ was modelled using the analytical model (Equation 2) by considering steady-flow conditions and the value of groundwater flux (q_2) applied during this second stage.

Figure 8a focuses on the temperature increase measured from t_0 to t_1, over which the flux (q_1) is constant. As the flow is constant during this period, the temperature evolution can be very well reproduced using the MILS model (Equation 2). Then, as shown in Figure 8b, the temperature increase measured from $t = t_1$ to $t = t_2$, over which the flux (q_2) is imposed, can be very well reproduced following the Equation 8 (black line).

Likewise, temperature increase measured from $t = t_2$ to $t = t_3$, over which the flux (q_3) is imposed, can be very well reproduced using the same superposition principle, as shown in Figure 8c (black line). Interestingly, this approach reproduces better the temperature reached at the end of this step than the direct use of the analytical solution for a single value of q (blue line). The comparison between these two lines confirms that the temperature stabilization is not completely reached at $t = t_3$. It would have required around 1.3 additional hours of heating to reach the steady-state and for the two curves to overlap.

Finally, the superposition principle is applied to model the temperature increase measured for $t > t_3$ under no-flow conditions ($q_4 = 0$ m.s^{-1}) (Figure 8d). Even if the model does not perfectly reproduce the temperature increase measured for $t > t_3$ (black line), the modelled curve remains satisfactory. The difference between the reproduced curve and experimental data can probably be explained, as discussed below, by experimental conditions and a longer heating period would certainly have improved the result.

Modelled curves in Figures 7 (black lines) correspond to curves that would be obtained for active-DTS measurements conducted under steady-flow conditions. It appears for q_1, q_2 and q_3, that temperature stabilization would be reached in approximatively 0.8 h, 4.8 h and 10.3 h. However, in the experiment, durations required to reach temperature stabilizations after flow changes were smaller: 4 h from q_1 to q_2 and 5.5 h from q_2 to q_3 (Figure 8b). This clearly shows that the duration of the transient period depends on the difference between the times required to reach stabilization for each flow value (4.8 h - 0.8 h for q varying between q_1 to q_2, and 10.3 h - 4.8 h for q varying between q_2 to q_3). This confirms that the duration of the transient temperature stage depends on both the value of the flow after the change, which controls the late behavior of the temperature elevation, and on the difference of fluxes before and after the flow change. Thus, for a flow change from q_1 to q_3, 9.5 h would be required to reach temperature stabilization while only 4h are required for fluxes varying from q_1 to q_2.

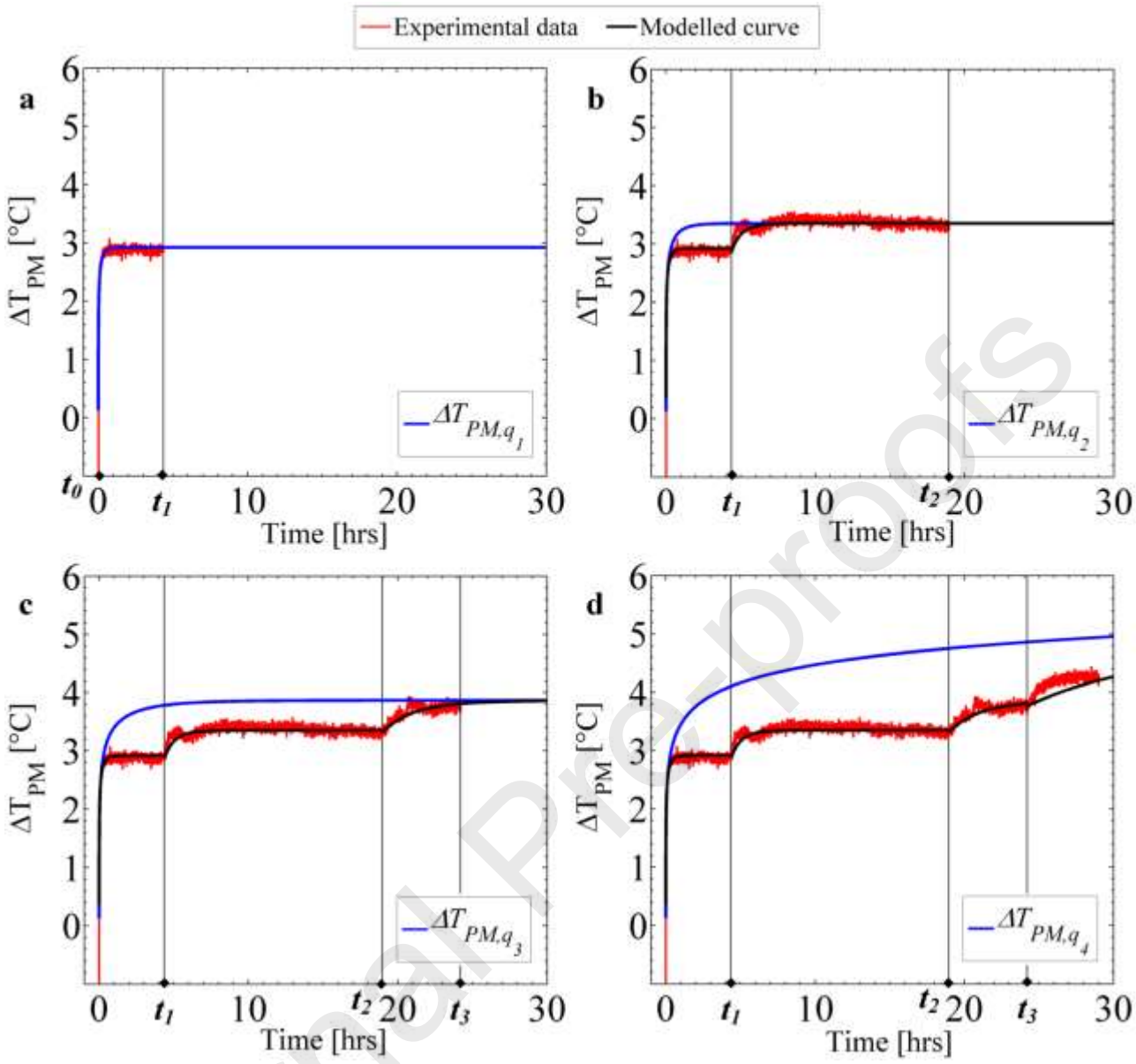

Figure 8. Step-by-step modeling of the temperature increase measured in the sandbox over the heating period (red line). Each plot (a,b,c,d) presents the temperature change associated to a flow change and the associated modelled curve (black line). For each step, the blue line corresponds to temperature increase modelled with the analytical model (Equation 2) considering the value of the groundwater flux applied at this step.

4. Discussions

In this study, we introduce active-DTS measurements as a new approach to continuously monitor groundwater fluxes changes over time. This approach allows to overcome the limitations of methods that have been proposed in the past decades for monitoring and quantifying the temporal dynamic of groundwater fluxes. We introduce the possibility of accurately estimating groundwater flow at high spatial resolution while continuously monitoring the temporal dynamics of groundwater flow at different time scales, including rapid flow fluctuations.

Both sandbox experiments and numerical simulations show that any changes in the flow rate instantaneously affect the temperature evolution, confirming that temperature elevation measured

during active-DTS measurements is sensitive to flow variations. Results are in perfect agreement with theoretical expectations. In the case of a change from flow-conditions to no-flow conditions, the temperature does not stabilize after the flow change and the time required for temperature to reach the conduction trend (Figure 5) can be very long (almost 24h in simulations). Numerical simulations were also made to simulate the effect of a flux increase on temperature response. Results are not presented here because they are very similar to results presented considering flux decrease. The only difference is that any flux increase induces a temperature decrease.

In addition, results show that if the flow change (either instantaneous or progressive) is followed by a steady-state flow period, the temperature tends to stabilize at late times. The temperature of stabilization exclusively depends on the effective groundwater flux at the time of the steady-state flow period and not on flow conditions or fluxes variations that have occurred in earlier times. Therefore, as soon as temperature steady state conditions are measured, the MILS model (Equation 2) or it simplified version (Equation 3) can be used to interpret the stabilization temperature and estimate the groundwater flux if the thermal conductivity value has been already determined.

However, in agreement with theoretical developments, results show that the thermal response to instantaneous flow changes is not instantaneous. A transient period is systematically observed in temperature evolution depending on the value of the groundwater flux. Despite this transient period, both sandbox experiments and numerical simulations confirm the possibility of modeling the thermal response resulting from an instantaneous flow change by applying the superposition principle (Eq. 8) and using the MILS model (Equation 2) considering the values of fluxes before and after the flow change. Thus, as demonstrated in Figure 8, the temperature evolution associated to several changes in flow-conditions can be modelled, which allows monitoring the temporal dynamic of fluxes, even if the temperature stabilization is not yet reached. This result is particularly promising because it suggests that an inverse model could be used reproduce temperature variations and assess flow variations over time. Note however that the flow change should be sufficiently important to induce a significant and measurable temperature change.

For any flow variation from q_1 to q_2, the duration of the temperature transient stage depends on the difference between the time required to reach the stabilization for q_2 under steady-flow conditions and the one required for q_1 under steady-flow conditions. Thus, the larger the difference between q_1 and q_2, the longer the time required to reach a new stable temperature stage. This is true for a flow decrease as well as for a flow increase.

For progressive flow changes, the flow quantification becomes limited as soon as steady thermal conditions are not reached. This can occur if the duration of temperature monitoring following the flow change is too short to reach temperature stabilization or if another flow change happens before the temperature stabilization. In this case, a qualitative characterization of flow dynamics is possible (a temperature increase resulting from flux decrease, and vice versa). Since the transient thermal stage cannot be modelled using the superposition principle introduced for modelling instantaneous flow changes, no flow quantification can be achieved as long as the temperature is not stabilized. In this case, a numerical model should be used to interpret the temperature elevation in order to reach a quantitative assessment of flow. This is probably what explains the difficulty for modeling temperature changes monitored during the sandbox experiment for $t > t_3$ (change from flow-conditions to no-flow conditions). In practice, reaching steady flow conditions after the stop of the water injection through the sandbox required some duration. It means that groundwater flow did not actually stop instantaneously, while the model considers no-flow conditions at $t=t_3$. A longer heating experiment would probably have permitted to improve modelling results.

Concerning periodic flow changes, the ability of monitoring groundwater fluxes variations depends on the difference between maximal and minimum fluxes, which controls the temperature changes rate and the time required to reach the maximum or minimum of temperature (Figure 6). If the difference of temperature stabilization times between the maximal flux and the minimum flux is shorter than the half period of the periodic flow change signal, the temperature change rate is comparable to the flow change rate. In this scale, the time shift between the temperature signal and the flow signal becomes negligible and flow variations can be monitored in real times. Minimal and maximal temperature recorded can be also used to interpret maximal and minimum water fluxes using the analytical solution (Equation 2) or its simplified version (Equation 3). On the opposite, if the difference of temperature stabilization times between the maximal flux and the minimum flux is larger than the half period of the periodic flow change signal, a time lag is observed between temperature variations and flow variations. Besides, in this case, the temperature signal appears attenuated in amplitude (Figure 6c and d) since the period of the signal is not long enough to reach maximal or minimum temperature. Thus, if the maximum and minimum temperatures recorded are interpreted using the analytical approach used in this study, minimal and maximal fluxes would be overestimated or underestimated. Once again, in this case, a numerical model could help for reproducing temperature variations and estimating the range of groundwater fluxes.

It should be also noted that we assume in this study that the ambient temperature of the porous media is steady over time. It involves that any temperature variations recorded is exclusively induced by the heating experiment. In practice, natural temperature variations can occur and affect the temperature signal measured during heating periods. This would be the case for instance if the method is used under losing stream conditions at the stream/aquifer interface, where stream temperature variations propagates in depth depending on downward water fluxes. It means that the temperature signal recorded during heating experiments should be processed in order to filter natural temperature variations before interpreting induced temperature variations. This point will be investigated in further works.

Conclusions

We investigated the potential of active-DTS measurements for characterizing variable groundwater fluxes. We demonstrated that temperature signal measured over time is sensitive to groundwater flow conditions and their temporal changes, offering very interesting perspectives to quantify and monitor fluxes variations. We showed in particular the ability of active-DTS measurements to monitor groundwater flow changes for different hydrological conditions. In complement to the few methods which allow quantifying groundwater flow variations, active-DTS measurements offer the possibility of characterizing fluxes at high spatial resolution, meaning that their use under transient flow conditions could allow to address the question of the characterization of both the spatial and the temporal variabilities of groundwater fluxes. In addition, results show that the method proposed in this study proved to be excellent for monitoring groundwater fluxes variations with a great accuracy.

These preliminary tests are particularly promising and open new perspectives for monitoring and/or quantifying the temporal dynamic of groundwater fluxes for many applications at different temporal scales. The approach seems particularly well suited to investigate flow fluctuations occurring over long time scales, for instance to study bank storage effects induced by square dam releases or recharge of highly heterogeneous systems, which are generally followed by relative long periods (few hours) of water levels stabilization (Ferencz et al. 2019). Likewise, the approach would be well suited for characterizing groundwater flow variations occurring over days (associated with precipitations for instance) or over weeks (seasonal fluctuations) since very low changes could be

quasi-continuously monitored. Active-DTS seems also very well suited to monitor groundwater fluxes at different depths during a pumping test that last few hours or days (Pouladi et al. 2021a) in order to image flow variability and sub-surface heterogeneities. The method should also be efficient to assess diurnal groundwater fluctuations resulting from evapotranspiration, atmospheric pressure effects or tidal effects for example. None other field method offers the possibility of quantifying both temporal and spatial variabilities of diurnal groundwater fluctuations.

Acknowledgments

The experimentation and the collaboration between the University of Rennes 1 and the University of Poitiers benefited from the support of INSU-CNRS through the Service National d'Observation H +. We thank Denis Paquet for helping us during the experimental work and Annick Battais for the computing support she provided.

Funding

This work was supported by the Agence de l'Eau Loire Bretagne and by the ANR project EQUIPEX CRITEX grant number ANR-11-EQPX-0011.

References

Abesser, C., F. Ciocca, J. Findlay, D. Hannah, P. Blaen, A. Chalari, M. Mondanos, and S. Krause. 2020. A distributed heat pulse sensor network for thermo-hydraulic monitoring of the soil subsurface. *Quarterly Journal of Engineering Geology and Hydrogeology* 53(3): 352–365. doi: 10.1144/qjegh2018-147.

Anderson, M. P. 2005. Heat as a ground water tracer. *Ground Water* 43(6): 951–968. doi: 10.1111/j.1745-6584.2005.00052.x.

Ataie-Ashtiani, B., R. E. Volker, and D. A. Lockington. 2001. Tidal effects on groundwater dynamics in unconfined aquifers. *Hydrological Processes* 15(4). John Wiley & Sons, Ltd: 655–669. doi: 10.1002/hyp.183.

Bakker, M., R. Calje, F. Schaars, K.-J. van der Made, and S. de Haas. 2015. An active heat tracer experiment to determine groundwater velocities using fiber optic cables installed with direct push equipment. *Water Resources Research* 51(4): 2760–2772. doi: 10.1002/2014WR016632.

Bense, V. F., T. Read, O. Bour, T. Le Borgne, T. Coleman, S. Krause, A. Chalari, M. Mondanos, F. Ciocca, and J. S. Selker. 2016. Distributed Temperature Sensing as a downhole tool in hydrogeology. *Water Resources Research* 52(12): 9259–9273. doi: 10.1002/2016WR018869.

Binley, A., S. S. Hubbard, J. A. Huisman, A. Revil, D. A. Robinson, K. Singha, and L. D. Slater. 2015. The emergence of hydrogeophysics for improved understanding of subsurface processes over multiple scales. *Water Resources Research* 51(6). John Wiley & Sons, Ltd: 3837–3866. doi: 10.1002/2015WR017016.

Boano, F., R. Revelli, and L. Ridolfi. 2013. Modeling hyporheic exchange with unsteady stream discharge and bedform dynamics. *Water Resources Research* 49(7). John Wiley & Sons, Ltd: 4089–4099. doi: 10.1002/wrcr.20322.

Boano, F., J. W. Harvey, A. Marion, A. I. Packman, R. Revelli, L. Ridolfi, and A. Wörman. 2014. Hyporheic flow and transport processes: Mechanisms, models, and biogeochemical implications. *Reviews of Geophysics* 52(4): 603–679. doi: 10.1002/2012RG000417.

Briggs, M. A., L. K. Lautz, J. M. McKenzie, R. P. Gordon, and D. K. Hare. 2012. Using high-resolution distributed temperature sensing to quantify spatial and temporal variability in vertical hyporheic flux. *Water Resources Research* 48(2). doi: 10.1029/2011WR011227.

Brouyère, S., J. Batlle-Aguilar, P. Goderniaux, and A. Dassargues. 2008. A new tracer technique for monitoring groundwater fluxes: The Finite Volume Point Dilution Method. *Journal of Contaminant Hydrology* 95(3): 121–140. doi: 10.1016/j.jconhyd.2007.09.001.

Brunner, P., R. Therrien, P. Renard, C. T. Simmons, and H.-J. H. Franssen. 2017. Advances in understanding river-groundwater interactions. *Reviews of Geophysics* 55(3): 818–854. doi: 10.1002/2017RG000556.

Burnett, W. C., P. K. Aggarwal, A. Aureli, H. Bokuniewicz, J. E. Cable, M. A. Charette, E. Kontar, S. Krupa, K. M. Kulkarni, A. Loveless, W. S. Moore, J. A. Oberdorfer, J. Oliveira, N. Ozyurt, P. Povinec, A. M. G. Privitera, R. Rajar, R. T. Ramessur, J. Scholten, T. Stieglitz, M. Taniguchi, and J. V. Turner. 2006. Quantifying submarine groundwater discharge in the coastal zone via multiple methods. *Science of The Total Environment* 367(2): 498–543. doi: 10.1016/j.scitotenv.2006.05.009.

Carslaw, H. S., and J. C. Jaeger. 1959. *Conduction of heat in solids*. Oxford Univers. Press.

Constantz, J. 2008. Heat as a tracer to determine streambed water exchanges. *Water Resources Research* 44(4). John Wiley & Sons, Ltd. doi: 10.1029/2008WR006996.

Diao, N., Q. Li, and Z. Fang. 2004. Heat transfer in ground heat exchangers with groundwater advection. *International Journal of Thermal Sciences* 43(12): 1203–1211. doi: 10.1016/j.ijthermalsci.2004.04.009.

Dimova, N. T., P. W. Swarzenski, H. Dulaiova, and C. R. Glenn. 2012. Utilizing multichannel electrical resistivity methods to examine the dynamics of the fresh water–seawater interface in two Hawaiian groundwater systems. *Journal of Geophysical Research: Oceans* 117(C2). John Wiley & Sons, Ltd. doi: 10.1029/2011JC007509.

Drost, W., D. Klotz, A. Koch, H. Moser, F. Neumaier, and W. Rauert. 1968. Point dilution methods of investigating ground water flow by means of radioisotopes. *Water Resources Research* 4(1): 125–146. doi: 10.1029/WR004i001p00125.

Ferencz, S. B., M. B. Cardenas, and B. T. Neilson. 2019. Analysis of the Effects of Dam Release Properties and Ambient Groundwater Flow on Surface Water-Groundwater Exchange Over a 100-km-Long Reach. *Water Resources Research* 55(11): 8526–8546. doi: 10.1029/2019WR025210.

Folch, A., L. del Val, L. Luquot, L. Martínez-Pérez, F. Bellmunt, H. Le Lay, V. Rodellas, N. Ferrer, A. Palacios, S. Fernández, M. A. Marazuela, M. Diego-Feliu, M. Pool, T. Goyetche, J. Ledo, P. Pezard, O. Bour, P. Queralt, A. Marcuello, J. Garcia-Orellana, M. W. Saaltink, E. Vázquez-Suñé, and J. Carrera. 2020. Combining fiber optic DTS, cross-hole ERT and time-lapse induction logging to characterize and monitor a coastal aquifer. *Journal of Hydrology* 588: 125050. doi: 10.1016/j.jhydrol.2020.125050.

Freeze, R., and J. Cherry. 1979. *GroundWater*. Vol. 16.

Freeze, R. A. 1974. Streamflow generation. *Reviews of Geophysics* 12(4). John Wiley & Sons, Ltd: 627–647. doi: 10.1029/RG012i004p00627.

Garcia-Orellana, J., V. Rodellas, J. Tamborski, M. Diego-Feliu, P. van Beek, Y. Weinstein, M. Charette, A. Alorda-Kleinglass, H. A. Michael, T. Stieglitz, and J. Scholten. 2021. Radium isotopes as submarine groundwater discharge (SGD) tracers: Review and recommendations. *Earth-Science Reviews* 220: 103681. doi: 10.1016/j.earscirev.2021.103681.

Ghasemizadeh, R., F. Hellweger, C. Butscher, I. Padilla, D. Vesper, M. Field, and A. Alshawabkeh. 2012. Review: Groundwater flow and transport modeling of karst aquifers, with particular reference to the North Coast Limestone aquifer system of Puerto Rico. *Hydrogeology Journal* 20(8): 1441–1461. doi: 10.1007/s10040-012-0897-4.

van de Giesen, N., S. C. Steele-Dunne, J. Jansen, O. Hoes, M. B. Hausner, S. Tyler, and J. Selker. 2012. Double-Ended Calibration of Fiber-Optic Raman Spectra Distributed Temperature Sensing Data. *Sensors* 12(5): 5471–5485. doi: 10.3390/s120505471.

de Graaf, I., T. Gleeson, L. Beek, E. Sutanudjaja, and M. Bierkens. 2019. Environmental flow limits to global groundwater pumping. *Nature* 574: 90–94. doi: 10.1038/s41586-019-1594-4.

Hancock, P. J. 2002. Human Impacts on the Stream–Groundwater Exchange Zone. *Environmental Management* 29(6): 763–781. doi: 10.1007/s00267-001-0064-5.

Harvey, J., and M. Gooseff. 2015. River corridor science: Hydrologic exchange and ecological consequences from bedforms to basins. *Water Resources Research* 51(9). John Wiley & Sons, Ltd: 6893–6922. doi: 10.1002/2015WR017617.

Hatch, C. E., A. T. Fisher, J. S. Revenaugh, J. Constantz, and C. Ruehl. 2006. Quantifying surface water-groundwater interactions using time series analysis of streambed thermal records: Method development. *Water Resources Research* 42(10): W10410. doi: 10.1029/2005WR004787.

Henderson, R. D., F. D. Day-Lewis, and C. F. Harvey. 2009. Investigation of aquifer-estuary interaction using wavelet analysis of fiber-optic temperature data. *Geophysical Research Letters* 36(6). John Wiley & Sons, Ltd. doi: 10.1029/2008GL036926.

Hermans, T., P. Goderniaux, D. Jougnot, J. Fleckenstein, P. Brunner, F. Nguyen, N. Linde, J. A. Huisman, O. Bour, J. Lopez Alvis, R. Hoffmann, A. Palacios, A.-K. Cooke, Á. Pardo-Álvarez, L. Blazevic, B. Pouladi, P. Haruzi, M. Kenshilikova, P. Davy, and T. Le Borgne. 2022. Advancing measurements and representations of subsurface heterogeneity and dynamic processes: towards 4D hydrogeology. *Hydrol. Earth Syst. Sci. Discuss.* 2022. Copernicus Publications: 1–55. doi: 10.5194/hess-2022-95.

Jamin, P., and S. Brouyère. 2018. Monitoring transient groundwater fluxes using the Finite Volume Point Dilution Method. *Journal of Contaminant Hydrology* 218: 10–18. doi: 10.1016/j.jconhyd.2018.07.005.

Jamin, P., P. Goderniaux, O. Bour, T. Le Borgne, A. Englert, L. Longuevergne, and S. Brouyère. 2015. Contribution of the finite volume point dilution method for measurement of groundwater fluxes

in a fractured aquifer. *Journal of Contaminant Hydrology* 182: 244–255. doi: 10.1016/j.jconhyd.2015.09.002.

Jiménez-Martínez, J., L. Longuevergne, T. Le Borgne, P. Davy, A. Russian, and O. Bour. 2013. Temporal and spatial scaling of hydraulic response to recharge in fractured aquifers: Insights from a frequency domain analysis. *Water Resources Research* 49(5). John Wiley & Sons, Ltd: 3007–3023. doi: 10.1002/wrcr.20260.

Keery, J., A. Binley, N. Crook, and J. W. N. Smith. 2007. Temporal and spatial variability of groundwater-surface water fluxes: Development and application of an analytical method using temperature time series. *Journal of Hydrology* 336(1–2): 1–16. doi: 10.1016/j.jhydrol.2006.12.003.

Kurylyk, B. L., D. J. Irvine, and V. F. Bense. 2019. Theory, tools, and multidisciplinary applications for tracing groundwater fluxes from temperature profiles. *Wiley Interdisciplinary Reviews: Water* 6(1): e1329. doi: 10.1002/wat2.1329.

Le Lay, H., Z. Thomas, F. Rouault, P. Pichelin, and F. Moatar. 2019. Characterization of Diffuse Groundwater Inflows into Stream Water (Part II: Quantifying Groundwater Inflows by Coupling FO-DTS and Vertical Flow Velocities). *Water* 11: 2430. doi: 10.3390/w11122430.

LeRoux, N. K., B. L. Kurylyk, M. A. Briggs, D. J. Irvine, J. J. Tamborski, and V. F. Bense. 2021. Using Heat to Trace Vertical Water Fluxes in Sediment Experiencing Concurrent Tidal Pumping and Groundwater Discharge. *Water Resources Research* 57(2). John Wiley & Sons, Ltd: e2020WR027904. doi: 10.1029/2020WR027904.

Lewandowski, J., S. Arnon, E. Banks, O. Batelaan, A. Betterle, T. Broecker, C. Coll, J. D. Drummond, J. Gaona Garcia, J. Galloway, J. Gomez-Velez, R. C. Grabowski, S. P. Herzog, R. Hinkelmann, A. Höhne, J. Hollender, M. A. Horn, A. Jaeger, S. Krause, A. Löchner Prats, C. Magliozzi, K. Meinikmann, B. B. Mojarrad, B. M. Mueller, I. Peralta-Maraver, A. L. Popp, M. Posselt, A. Putschew, M. Radke, M. Raza, J. Riml, A. Robertson, C. Rutere, J. L. Schaper, M. Schirmer, H. Schulz, M. Shanafield, T. Singh, A. S. Ward, P. Wolke, A. Wörman, and L. Wu. 2019. Is the Hyporheic Zone Relevant beyond the Scientific Community? *Water* 11(11). doi: 10.3390/w11112230.

Lin, Y.-F., C.-H. Chang, and J.-P. Tsai. 2022. Analytical solution for estimating transient vertical groundwater flux from temperature-depth profiles. *Journal of Hydrology* 610: 127920. doi: 10.1016/j.jhydrol.2022.127920.

Matheswaran, K., M. Blemmer, D. Rosbjerg, and E. Boegh. 2014. Seasonal variations in groundwater upwelling zones in a Danish lowland stream analyzed using Distributed Temperature Sensing (DTS). *Hydrological Processes* 28(3): 1422–1435. doi: 10.1002/hyp.9690.

McClain, M. E., E. W. Boyer, C. L. Dent, S. E. Gergel, N. B. Grimm, P. M. Groffman, S. C. Hart, J. W. Harvey, C. A. Johnston, E. Mayorga, W. H. McDowell, and G. Pinay. 2003. Biogeochemical Hot Spots and Hot Moments at the Interface of Terrestrial and Aquatic Ecosystems. *Ecosystems* 6(4): 301–312. doi: 10.1007/s10021-003-0161-9.

Munn, J. D., C. H. Maldaner, T. I. Coleman, and B. L. Parker. 2020. Measuring Fracture Flow Changes in a Bedrock Aquifer Due to Open Hole and Pumped Conditions Using Active Distributed

Temperature Sensing. *Water Resources Research* 56(10). John Wiley & Sons, Ltd: e2020WR027229. doi: 10.1029/2020WR027229.

Paepen, M., D. Hanssens, P. De Smedt, K. Walraevens, and T. Hermans. 2020. Combining resistivity and frequency domain electromagnetic methods to investigate submarine groundwater discharge in the littoral zone. *Hydrology and Earth System Sciences* 24(7): 3539–3555. doi: 10.5194/hess-24-3539-2020.

Pitrak, M., S. Mares, and M. Kobr. 2007. A Simple Borehole Dilution Technique in Measuring Horizontal Ground Water Flow. *Groundwater* 45(1). John Wiley & Sons, Ltd: 89–92. doi: 10.1111/j.1745-6584.2006.00258.x.

Pouladi, B., N. Linde, L. Longuevergne, and O. Bour. 2021a. Individual and joint inversion of head and flux data by geostatistical hydraulic tomography. *Advances in Water Resources* 154: 103960. doi: 10.1016/j.advwatres.2021.103960.

Pouladi, B., O. Bour, L. Longuevergne, J. de La Bernardie, and N. Simon. 2021b. Modelling borehole flows from Distributed Temperature Sensing data to monitor groundwater dynamics in fractured media. *Journal of Hydrology* 598: 126450. doi: 10.1016/j.jhydrol.2021.126450.

Rau, G. C., M. S. Andersen, A. M. McCallum, H. Roshan, and R. I. Acworth. 2014. Heat as a tracer to quantify water flow in near-surface sediments. *Earth-Science Reviews* 129: 40–58. doi: 10.1016/j.earscirev.2013.10.015.

Read, T., O. Bour, J. S. Selker, V. F. Bense, T. L. Borgne, R. Hochreutener, and N. Lavenant. 2014. Active-distributed temperature sensing to continuously quantify vertical flow in boreholes. *Water Resources Research* 50(5). John Wiley & Sons, Ltd: 3706–3713. doi: 10.1002/2014WR015273.

Robinson, C. E., P. Xin, I. R. Santos, M. A. Charette, L. Li, and D. A. Barry. 2018. Groundwater dynamics in subterranean estuaries of coastal unconfined aquifers: Controls on submarine groundwater discharge and chemical inputs to the ocean. *Advances in Water Resources* 115: 315–331. doi: 10.1016/j.advwatres.2017.10.041.

Sayde, C., C. K. Thomas, J. Wagner, and J. Selker. 2015. High-resolution wind speed measurements using actively heated fiber optics. *Geophysical Research Letters* 42(22): 10064–10073. doi: 10.1002/2015GL066729.

Sebok, E., C. Duque, J. Kazmierczak, P. Engesgaard, B. Nilsson, S. Karan, and M. Frandsen. 2013. High-resolution distributed temperature sensing to detect seasonal groundwater discharge into Lake Vaeng, Denmark. *Water Resources Research* 49(9): 5355–5368. doi: 10.1002/wrcr.20436.

Selker, F., and J. S. Selker. 2018. Investigating Water Movement Within and Near Wells Using Active Point Heating and Fiber Optic Distributed Temperature Sensing. *Sensors* 18(4): 1023. doi: 10.3390/s18041023.

Selker, J. S., L. Thevenaz, H. Huwald, A. Mallet, W. Luxemburg, N. van de Giesen, M. Stejskal, J. Zeman, M. Westhoff, and M. B. Parlange. 2006. Distributed fiber-optic temperature sensing for hydrologic systems. *Water Resources Research* 42(12): W12202. doi: 10.1029/2006WR005326.

Shanafield, M., E. W. Banks, J. W. Arkwright, and M. B. Hausner. 2018. Fiber-Optic Sensing for Environmental Applications: Where We Have Come From and What Is Possible. *Water Resources Research* 54(11): 8552–8557. doi: 10.1029/2018WR022768.

Simon, N., O. Bour, N. Lavenant, G. Porel, B. Nauleau, B. Pouladi, and L. Longuevergne. 2020. A Comparison of Different Methods to Estimate the Effective Spatial Resolution of FO-DTS Measurements Achieved during Sandbox Experiments. *Sensors* 20(2): 570. doi: 10.3390/s20020570.

Simon, N., O. Bour, N. Lavenant, G. Porel, B. Nauleau, B. Pouladi, L. Longuevergne, and A. Crave. 2021. Numerical and Experimental Validation of the Applicability of Active-DTS Experiments to Estimate Thermal Conductivity and Groundwater Flux in Porous Media. *Water Resources Research* 57(1). John Wiley & Sons, Ltd: e2020WR028078. doi: 10.1029/2020WR028078.

Simon, N., O. Bour, M. Faucheux, N. Lavenant, H. Le Lay, O. Fovet, Z. Thomas, and L. Longuevergne. 2022. Combining passive and active distributed temperature sensing measurements to locate and quantify groundwater discharge variability into a headwater stream. *Hydrology and Earth System Sciences* 26(5): 1459–1479. doi: 10.5194/hess-26-1459-2022.

Slater, L. D., D. Ntarlagiannis, F. D. Day-Lewis, K. Mwakanyamale, R. J. Versteeg, A. Ward, C. Strickland, C. D. Johnson, and J. W. Lane. 2010. Use of electrical imaging and distributed temperature sensing methods to characterize surface water-groundwater exchange regulating uranium transport at the Hanford 300 Area, Washington. *Water Resources Research* 46: W10533. doi: 10.1029/2010WR009110.

Taniguchi, M., H. Dulai, K. M. Burnett, I. R. Santos, R. Sugimoto, T. Stieglitz, G. Kim, N. Moosdorf, and W. C. Burnett. 2019. Submarine Groundwater Discharge: Updates on Its Measurement Techniques, Geophysical Drivers, Magnitudes, and Effects. *Frontiers in Environmental Science* 7: 141. doi: 10.3389/fenvs.2019.00141.

des Tombe, B. F., M. Bakker, F. Smits, F. Schaars, and K.-J. van der Made. 2019. Estimation of the Variation in Specific Discharge Over Large Depth Using Distributed Temperature Sensing (DTS) Measurements of the Heat Pulse Response. *Water Resources Research* 55(1): 811–826. doi: 10.1029/2018WR024171.

Tyler, S. W., J. S. Selker, M. B. Hausner, C. E. Hatch, T. Torgersen, C. E. Thodal, and S. G. Schladow. 2009. Environmental temperature sensing using Raman spectra DTS fiber-optic methods. *Water Resources Research* 45: W00D23. doi: 10.1029/2008WR007052.

del Val, L., J. Carrera, M. Pool, L. Martínez, C. Casanovas, O. Bour, and A. Folch. 2021. Heat Dissipation Test With Fiber-Optic Distributed Temperature Sensing to Estimate Groundwater Flux. *Water Resources Research* 57(3). John Wiley & Sons, Ltd: e2020WR027228. doi: 10.1029/2020WR027228.

Winter, T., J. Harvey, O. Franke, and W. Alley. 1998. Ground water and surface water a single resource. *U.S. Geol. Surv. Circ.* 1139.

CRediT statements

Nataline Simon : Conceptualization, Methodology, Software, Validation, Formal analysis, Investigation, Writing - Original Draft, Writing - Review & Editing, Visualization **Olivier Bour** : Conceptualization, Methodology, Resources, Writing - Review & Editing, Supervision, Project administration, Funding acquisition **Nicolas Lavenant** : Investigation, Resources **Gilles Porel** : Investigation, Resources, Funding acquisition **Benoît Nauleau** : Investigation, Resources **Maria Klepikova** : Writing - Review & Editing

Highlights

- Active-DTS methods are well suited for monitoring groundwater flows variations
- Temperature evolution during heating experiment is sensitive to fluxes variations
- Groundwater fluxes dynamic can be characterized at different temporal scales